

Closed-form expressions for particle relative velocities induced by turbulence (Research Note)

C. W. Ormel¹ and J. N. Cuzzi²

¹ Kapteyn Astronomical Institute, University of Groningen, PO box 800, 9700 AV Groningen, The Netherlands
e-mail: ormel@astro.rug.nl

² Ames Research Center, NASA, Mail Stop 245-3, Moffett Field, CA 94035, USA
e-mail: jcuzzi@mail.arc.nasa.gov

Received 8 December 2006 / Accepted 1 February 2007

ABSTRACT

In this note we present complete, closed-form expressions for random relative velocities between colliding particles of arbitrary size in nebula turbulence. These results are exact for very small particles (those with stopping times much shorter than the large eddy overturn time) and are also surprisingly accurate in complete generality (that is, also apply for particles with stopping times comparable to, or much longer than, the large eddy overturn time). We note that some previous studies may have adopted previous simple expressions, which we find to be in error regarding the size dependence in the large particle regime.

Key words. turbulence – dust, extinction – planetary systems: protoplanetary disks

1. Introduction and outline

Gas in astrophysical environments is often in a turbulent state of motion, constantly affected by temporally and spatially varying accelerations from eddies having a variety of scales. A particle, due to its inertia, does not instantaneously follow the gas motions but requires a certain time in order to align with the gas motion. The particle's interaction with the gas is captured in the definition of the *stopping time* of the particle (sometimes also referred to as friction time),

$$t_s = \frac{3}{4} \frac{m}{c_g \rho_g \sigma}, \quad (1)$$

where c_g and ρ_g are, respectively, the sound speed and the volume mass density of the gas, and m and σ the mass and projected surface area of the particle. Due to this inertial lag, a particle develops a relative velocity with respect to the gas. In addition, these lags also cause particles to acquire relative velocities among themselves.

While the general problem of calculating these relative velocities has received considerable attention in the basic fluid dynamics community (see Cuzzi & Hogan 2003, for references; henceforth CH03), the formalism most frequently used in the astrophysics community was developed by Völk et al. (1980) and Markiewicz et al. (1991, henceforth MMV). In these works the final results are given in terms of integrals that were not *solved* analytically. Some workers have used simple fits to these numerical results in their models of dust coagulation; however, simple closed-form expressions for particle-particle relative velocities would help streamline these models (e.g. Suttner & Yorke 2001; Dullemond & Dominik 2005; Nomura & Nakagawa 2006; Ormel et al. 2007). Recently, CH03 obtained closed-form expressions from the MMV model for particle velocities in inertial space V_p , for particle-gas relative velocities V_{pg} , and for relative velocities between two identical particles V_{pp} , but did not

extend their results to the general case of two particles of different stopping times. Moreover, CH03 stressed the validity of their analytical results for particles with stopping times much shorter than the large eddy turnover time. In this note we generalize the approach and results of CH03 to obtain closed-form expressions for relative velocities between particles of arbitrary, and unequal, size. In Sect. 2 we define important quantities and review previous work. In Sect. 3 we present two independent approaches for obtaining the desired closed-form solutions. In Sect. 4 we give our conclusions and a summary.

2. Definitions and previous work

Nebula gas turbulence is generally described as being composed of eddies having a range of spatial scales ℓ and spatial frequencies $k = 1/\ell$, with an energy spectrum $E(k) \propto k^{-5/3}$ and total energy $V_g^2/2$ per unit mass providing the normalization condition

$$\frac{V_g^2}{2} = \int_{k_L}^{k_\eta} dk E(k), \quad (2)$$

from which $E(k) = V_g^2/3k_L (k/k_L)^{-5/3}$. The largest, or integral scale, eddies have spatial scale $L = 1/k_L$, and the smallest, or Kolmogorov scale, eddies have spatial scale $\eta = 1/k_\eta$. The form of $E(k)$ given above is the inertial range expression most often assumed, with $E(k) = 0$ for $k > k_\eta$ or $k < k_L$. Völk et al. (1980) used a spectrum $P(k) = 2E(k)$ and stipulated no smallest scale η for the turbulence, but Weidenschilling (1984) and MMV noted that a finite value for $\eta > 0$ had profound effects on the particle velocities, especially the relative velocities V_{pp} for small particles. Each eddy wavenumber k has a characteristic velocity $V(k) = \sqrt{2kE(k)}$ and overturn time $t_k = \ell/V(k) = (kV(k))^{-1}$. Our standard definition of the particle *Stokes number* is $St = t_s/t_L$, where t_L is the overturn time of the largest eddy, generally taken

to be the local orbit period. The local turbulent intensity is described by its Reynolds number, Re , defined as the ratio between the turbulent and the molecular kinematic viscosities, $Re = \nu_T/\nu$. The values for ℓ , ν and t at the integral scale then follow from Re , e.g., $\eta = Re^{-3/4}L$ and $t_\eta = Re^{-1/2}t_L$. These expressions bring Re into the final expressions for particle velocities as a limit on certain integrals (cf. CH03 for more detail). In the notation of astrophysical “ α -models”, $Re = \alpha c_g H_g/\nu = \alpha c_g^2/\nu\Omega$ where c_g , H_g , and ν are the sound speed, vertical scale height, and kinematic viscosity of the nebula gas and Ω is the orbital frequency.

Völk et al. (1980) introduced the concept of “eddy classes”. Class I eddies vary slowly enough that a particle, upon entering a class I eddy, will forget its initial motion and align itself to the gas motions of the eddy before the eddy decays or the particle leaves the eddy. Class II eddies, on the other hand, have fluctuation times shorter than the particle’s stopping time t_s , and fluctuate too rapidly to provide more than a small perturbation on the particle. The timescale on which an eddy decays is given by t_k , while the eddy-crossing timescale is $t_{\text{cross}} \approx \ell/V_{\text{rel}} = (kV_{\text{rel}}(k))^{-1}$, with V_{rel} the relative velocity between a grain and an eddy. For an eddy to be of class I both t_k and t_{cross} must be larger than the particle’s stopping time. The boundary between these classes occurs at $k = k^*$ (or at $t_k = t^*$) which can be defined as (Völk et al. 1980, MMV):

$$\frac{1}{t_s} = \frac{1}{t^*} + \frac{1}{t_{\text{cross}}} = \frac{1}{t^*} + k^* V_{\text{rel}}(k^*). \quad (3)$$

It is important to realize that k^* (or t^*) is a function of stopping time t_s , that is, the boundary separating the two classes is different for each particle. The different treatment for the two eddy classes $k < k^*$ and $k > k^*$ forms the core of the derivation of the turbulence-induced particle velocities.

All turbulent velocities in this note are statistical, root-mean-square, averaged quantities. The average inertial space particle velocity V_p is given by Eq. (6) of MMV.

$$V_p^2 = \int_{k_L}^{\max(k^*, k_L)} dk 2E(k) (1 - K^2) + \int_{\max(k^*, k_L)}^{k_\eta} dk 2E(k) (1 - K) [g(\chi) + Kh(\chi)], \quad (4)$$

in which $K = t_s/(t_s + t_k)$. The K^2 term in the first integral results from the more recently preferred “ $n = 1$ ” gas velocity autocorrelation function (MMV and CH03). The functions $g(\chi) = \chi^{-1} \tan^{-1}(\chi)$ and $h(\chi) = 1/(1 + \chi^2)$ with $\chi = Kt_k k V_{\text{rel}}$ were first obtained by Völk et al. (1980).

CH03 noted that, for very small particles with $t_s \ll t_L$ or $St \ll 1$, the second integral becomes negligible, leaving only the first integral which is analytically solvable and for which the upper limit can be extended to k_η with negligible error. Here, to generalize the approach of CH03 to particles of *arbitrary* size, we approximate $h(\chi) = g(\chi) = 1$ for *all* particle sizes (see CH03 Sect. 2.2.3 for supporting logic). Numerical calculations of $h(\chi)$ and $g(\chi)$ validate this approximation to order unity (see Appendix A), and we gain further confidence in it from a posteriori comparison with exact numerical model results. The general expression for V_p^2 is then the same as in the $t_s \ll t_L$ regime, and the same analytical result is obtained, i.e. CH03,

$$V_p^2 = \int_{k_L}^{k_\eta} dk 2E(k) (1 - K^2) \quad (5)$$

$$= V_g^2 \left(1 - \frac{St^2(1 - Re^{-1/2})}{(St + 1)(St + Re^{-1/2})} \right). \quad (6)$$

CH03 did not give this explicit result for V_p , but merely noted that it was straightforward to derive it from their Eq. (19) for V_{pg} and the general relationship $V_{pg}^2 = V_p^2 - V_g^2$; however we will use it explicitly here.

Comparison of the predictions of this simple expression with detailed numerical results (MMV, CH03) show that it is indeed a good approximation for arbitrary St . A more accurate approximation to Eq. (4), in which the g and h functions are approximated as power-laws in k^*/k , is outlined in Appendix A. Unless $St \ll 1$, we can neglect the Reynolds number term in Eq. (6) and obtain $V_p = V_g/\sqrt{1 + St}$, a well known result (Völk et al. 1980; Cuzzi et al. 1993; Schräpler & Henning 2004) which describes the diffusivity of large particles in turbulence.

3. Results

3.1. k -space approach

MMV (their Eq. (7)) expressed the relative velocities $V_{p_1 p_2}$ between particles of different stopping times t_1 and t_2 as

$$V_{p_1 p_2}^2 = V_{p_1}^2 + V_{p_2}^2 - 2\overline{V_{p_1} V_{p_2}} \equiv \Delta V_{12}^2. \quad (7)$$

Having already derived $V_{p_i}^2$ ($i = 1, 2$) above, we can determine ΔV_{12} by evaluating the cross term $\overline{V_{p_1} V_{p_2}}$; this paper presents analytical solutions of this problem obtained in two separate ways. In this subsection we retain the wavenumber dependence; in the next subsection we transform to time variables. In Eq. (8) of MMV the cross term is given as a sum over the two particle sizes involved, which we separate here, writing $\Delta V_{12}^2 = V_{p_1}^2 + V_{p_2}^2 - (V_{c_1}^2 + V_{c_2}^2)$, where

$$V_{c_i}^2 = \frac{2t_i}{t_1 + t_2} \left(\int_{k_L}^{\min(k_1^*, k_2^*)} E(k) dk - \int_{k_L}^{\min(k_1^*, k_2^*)} E(k) \left(\frac{1}{1 + t_k/t_i} \right)^2 dk \right). \quad (8)$$

Changing variable to $x = k/k_L$, substituting for $E(k)$, and converting stopping time t_i to Stokes number $St_i = t_i/t_L$:

$$V_{c_i}^2 = \frac{2V_g^2 t_i}{3(t_1 + t_2)} \left[\int_1^{x_1^*} x^{-5/3} dx - \int_1^{x_1^*} \frac{St_i^2 dx}{x^{5/3}(St_i + x^{-2/3})^2} \right], \quad (9)$$

where we have taken, without loss of generality, $k_1^* \leq k_2^*$. The first integral is trivial and the second integral can be solved exactly as in Eqs. (17)–(19) of CH03. In evaluating the specific value of the integrals above, we need a closed form for the upper limit $x_1^* = k_1^*/k_L$. A simple prescription is readily found by inspection of Fig. 3 of CH03: $x_1^* = k_1^*/k_L = 0.5St_1^{-3/2} + 1$. That is, the boundary eddy for particles with stopping time t_1 is that for which $t_k \sim t_1$ until $t_1 > t_L$, beyond which it remains constant. This is merely a convenient mathematical shorthand to keep everything in closed form. Then, repeating the analytical solution of CH03 (Eqs. (17)–(19)) we obtain

$$V_{c_i}^2 = V_g^2 \frac{t_i}{(t_1 + t_2)} \left[\left(1 - x_1^{*-2/3} \right) - \left(\frac{St_i}{1 + St_i} - \frac{St_i}{1 + St_i x_1^{*2/3}} \right) \right]. \quad (10)$$

This solution for the cross term is easily combined with Eq. (6) to obtain expressions for particle-particle relative velocities ΔV_{12}^2 . Further manipulation of these expressions may be possible, but the important point here is that ΔV_{12} can be expressed in

closed form as function of St_1 , St_2 , V_g , and Re . With a few minutes of algebra, simpler expressions can be found in the limiting regimes of interest ($St_1 \ll 1, \gg 1$, etc.) which agree well with those which we present in the next section, for analytical solutions obtained in the time domain instead of the wavenumber domain, and where an analytical solution for the boundary $k^*(t^*)$ is used rather than the form for x_1^* adopted above. It should be recalled that, for *very* small particles $t_s < t_\eta$, x_1^* has an upper limit of $k_\eta/k_L = Re^{3/4}$ (see, e.g. CH03 Fig. 3).

3.2. t -space approach

The integrals expressing V_{pi}^2 and V_{ci}^2 are transformed into a simpler form by changing variables from k to t_k . Since $t_k = 1/kV(k) = (k\sqrt{2kE(k)})^{-1}$ and $E(k) = Ak^{-5/3}$ for a Kolmogorov power spectrum (where A is the normalization factor), we obtain that $E(k)dk = \frac{3}{2}\sqrt{2}A^{3/2}dt_k$. Now, $A = \frac{1}{3}V_g^2k_L^{2/3}$ from the normalization of the turbulent spectrum (Eq. (2)), $k_L = (V_L t_L)^{-1}$ with V_L the velocity of the largest eddy, and $V_L^2 = \frac{2}{3}V_g^2$ also by normalizing the power spectrum (see CH03). We then end up with

$$E(k) dk = \frac{1}{2} \frac{V_g^2}{t_L} dt_k, \quad (11)$$

which can be substituted into all the integrals, putting them into a simpler form. For instance, Eq. (5) becomes for particle i

$$V_{pi}^2 = \frac{V_g^2}{t_L} \int_{t_\eta}^{t_L} dt_k \left(1 - \left(\frac{t_i}{t_i + t_k} \right)^2 \right) = \frac{V_g^2}{t_L} \left[t_k + \frac{t_i^2}{t_i + t_k} \right]_{t_\eta}^{t_L}. \quad (12)$$

Similarly, the cross term becomes

$$V_{ci}^2 = \frac{V_g^2}{t_L} \frac{2t_i}{t_1 + t_2} \int_{t_{12}^*}^{t_L} dt_k \left(1 - \left(\frac{t_i}{t_i + t_k} \right)^2 \right) \quad (13)$$

$$= \frac{V_g^2}{t_L} \frac{2t_i}{t_1 + t_2} \left[t_k + \frac{t_i^2}{t_i + t_k} \right]_{t_{12}^*}^{t_L}. \quad (14)$$

With $t_{12}^* = \max(t_1^*, t_2^*)$ and $t_\eta \leq t_{12}^* \leq t_L$ since t^* refers to an eddy's turn-over time. We now solve for ΔV_{12}^2 by splitting the integral in Eq. (12) at t_{12}^* and subtract the corresponding V_{ci} terms from Eq. (14) to get

$$\Delta V_{12}^2 = \frac{V_g^2}{t_L} \left(\left[t_k + \frac{t_1^2}{t_1 + t_k} \right]_{t_\eta}^{t_{12}^*} + \left[t_k + \frac{t_1^2}{t_1 + t_k} \right]_{t_{12}^*}^{t_L} - \frac{2t_1}{t_1 + t_2} \left[t_k + \frac{t_1^2}{t_1 + t_k} \right]_{t_{12}^*}^{t_L} + (1 \leftrightarrow 2) \right), \quad (15)$$

where the $(1 \leftrightarrow 2)$ symbol indicates interchange between particles 1 and 2. With further manipulation and cancellation of terms, the previous expression simplifies slightly to

$$\Delta V_{12}^2 = \frac{V_g^2}{t_L} \left(\left[t_k + \frac{t_1^2}{t_1 + t_k} \right]_{t_\eta}^{t_{12}^*} + \frac{t_2 - t_1}{t_1 + t_2} \left[\frac{t_1^2}{t_1 + t_k} \right]_{t_{12}^*}^{t_L} + (1 \leftrightarrow 2) \right) = \Delta V_{II}^2 + \Delta V_I^2. \quad (16)$$

This is perhaps the most concise way to write the expressions for ΔV_{12}^2 . The first term we call ΔV_{II}^2 since this term involves class II (fast) eddies. If $t_{12}^* = t_L$ (heavy particles) all eddies are fast and only this term remains. Conversely, if $t_{12}^* = t_\eta$ (small particles) the contribution from ΔV_{II} vanishes and the second term, ΔV_I ,

determines relative velocities. In the intermediate regime, $t_\eta < t_{12}^* < t_L$, both terms contribute. Written in terms of the Stokes numbers these terms becomes

$$\Delta V_I^2 \equiv \frac{V_g^2}{t_L} \frac{t_2 - t_1}{t_1 + t_2} \left[\frac{t_1^2}{t_1 + t_k} \right]_{t_{12}^*}^{t_L} + (1 \leftrightarrow 2) = V_g^2 \frac{St_1 - St_2}{St_1 + St_2} \left(\frac{St_1^2}{St_{12}^* + St_1} - \frac{St_1^2}{1 + St_1} - (1 \leftrightarrow 2) \right) \quad (17)$$

$$\Delta V_{II}^2 \equiv \frac{V_g^2}{t_L} \left[t_k + \frac{t_1^2}{t_1 + t_k} \right]_{t_\eta}^{t_{12}^*} + (1 \leftrightarrow 2) = V_g^2 \left((St_{12}^* - Re^{-1/2}) + \frac{St_1^2}{St_1 + St_{12}^*} - \frac{St_1^2}{St_1 + Re^{-1/2}} + (1 \leftrightarrow 2) \right). \quad (18)$$

Note again that since $t_\eta \leq t_{12}^* \leq t_L$ we also have that $Re^{-1/2} \leq St_{12}^* \leq 1$. Below, we will first solve for St_{12}^* , and then consider solutions for ΔV_{12} in various limiting cases of the particle stopping times.

3.2.1. Solving for t^*

The relative velocity between a particle with stopping time t_s and an eddy k , is given by Völk et al. (1980), Eq. (15):

$$V_{rel}(k)^2 = V_o^2 + 2 \int_{k_L}^k dk' E(k') \left(\frac{t_s}{t_s + t_k} \right)^2. \quad (19)$$

V_o is any systematic velocity component not driven by turbulence – such as due to pressure-gradient driven azimuthal headwind, the ensuing radial drift, or vertical settling under solar gravity. We can integrate this equation in the same fashion as Eq. (14) and arrive at

$$V_{rel}(k^*)^2 = V_o^2 + \frac{V_g^2}{t_L} \left[\frac{t_s^2}{t_s + t_k} \right]_{t_L}^{t^*} = V_o^2 + \frac{V_g^2 t_s}{t_L} \left(\frac{1}{1 + y^*} - \frac{1}{1 + y_L} \right), \quad (20)$$

in which $y = t_k/t_s$. Also, using the definition for t_k (see text above Eq. (11)), k^* can be expressed as $(k^*)^2 = (2A)^{-3/2} t^{*-3} = \frac{3}{2} V_g^{-2} t_L t^{*-3}$. Inserting the expressions for k^* and V_{rel}^2 into Eq. (3), assuming that $V_o = 0$ for simplicity (see however Sect. 3.3), we obtain:

$$\frac{1}{k^*} \left(\frac{1}{t_s} - \frac{1}{t^*} \right) = V_{rel} \Rightarrow \quad (21a)$$

$$t^* \left(\frac{t^*}{t_s} - \frac{t^*}{t^*} \right)^2 = (2A)^{-3/2} V_{rel}^2 \Rightarrow \quad (21b)$$

$$t^* (y^* - 1)^2 = \frac{3}{2} t_s \left(\frac{1}{1 + y^*} - \frac{1}{1 + y_L} \right) \Rightarrow \quad (21c)$$

$$\frac{2}{3} y^* (y^* - 1)^2 - \frac{1}{1 + y^*} = -\frac{1}{1 + y_L}, \quad (21d)$$

where we have defined $y^* = t^*/t_s$ and $y_L = t_L/t_s = St^{-1}$. The LHS of Eq. (21d) is plotted in Fig. 1. If $y_L \gg 1$ for small particles, the RHS of Eq. (21d) is negligible and the numerical solution for y^* becomes $y^* \approx y_a^* = 1.6$, or $t^* \approx 1.6t_s$. On the other

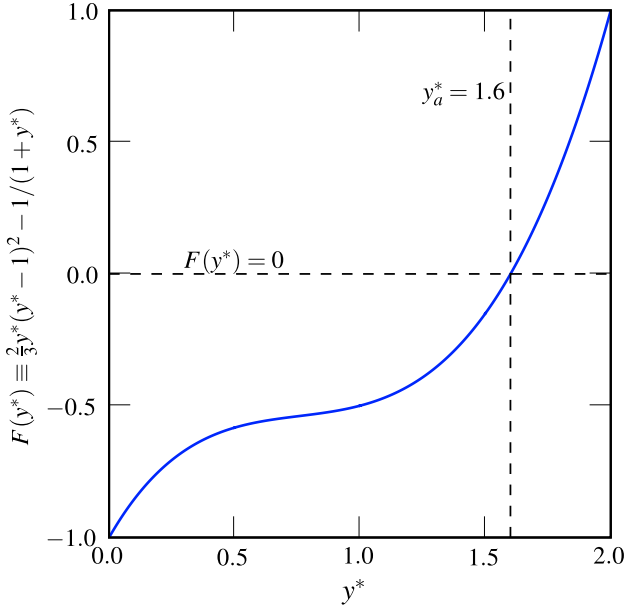


Fig. 1. The function $\frac{2}{3}y^*(y^*-1)^2 - 1/(1+y^*)$. If $t_s \ll t_L$ and $V_o = 0$ (no systematic velocity drifts; see Sect. 3.3) this equation is equal to zero and we find a solution $y^* = t^*/t_s \approx y_a^* = 1.6$. On the other hand, for $t_s \sim t_L$, the RHS of Eq. (21d) is ≈ -0.5 and $y^* \approx 1$.

hand, when t_s nears t_L , the $-1/(1+y_L)$ term causes the RHS of Eq. (21d) to drop to -0.5 , and $y^* \rightarrow 1$. For $t_s > t_L$ we always have that $t^* = t_L$; i.e., for such a particle all eddies are of class 2. In Fig. 2 we compare the exact solution (dashed line) for t^* with the $t^* \approx y_a^* t_s = 1.6 t_s$ approximation (solid line; in both cases $t^* \leq t_L$ is simply enforced), and the empirical function $k^*/k_L = 1 + \frac{1}{2}St^{-3/2}$ (dotted line; see Sect. 3.1).

The exact solution for ΔV_{12} (Eq. (16)) is given in Fig. 3 both for $t_1 \gg t_2$ (solid curve) and for particles of equal stopping times (dashed curve). A Reynolds number of $Re = 10^8$ has been adopted.

3.3. The role of V_o : eddy-crossing effects

Systematic velocities V_o due to vertical settling, and pressure-gradient headwinds and drifts, will occur (e.g. Nakagawa et al. (1986)). Because particles drift through eddies, their transit time is affected (because V_{rel} is larger) and the boundary between class I and II eddies shifts. Cuzzi et al. (1993) include this effect, due to vertical settling, in their model of particle diffusion (their Eq. (43)). The model presented here offers a generalized way of treating this effect, which we will only sketch here.

Repeating the procedure outlined in Sect. 3.2.1 but retaining the V_o term in V_{rel} (Eq. (20)), we end up with Eq. (21d) including a correction term

$$\frac{2}{3}y^*(y^*-1)^2 - \frac{1}{1+y^*} \equiv F(y^*) = -\frac{St}{1+St} + \frac{1}{St} \frac{V_o^2}{V_g^2}, \quad (22)$$

where we have substituted $St = 1/y_L$. The correction term can be roughly constrained using an estimate of the systematic drift velocity $V_o \sim (St/(St+1))\beta V_K$, where V_K is the Keplerian velocity at distance a from the Sun, Ω is the orbit frequency, and $\beta = (H_g/a)^2$ is a radial pressure gradient parameter; also we take $V_g = \alpha^{1/2}c_g$ (see, e.g., Nakagawa et al. 1986 or

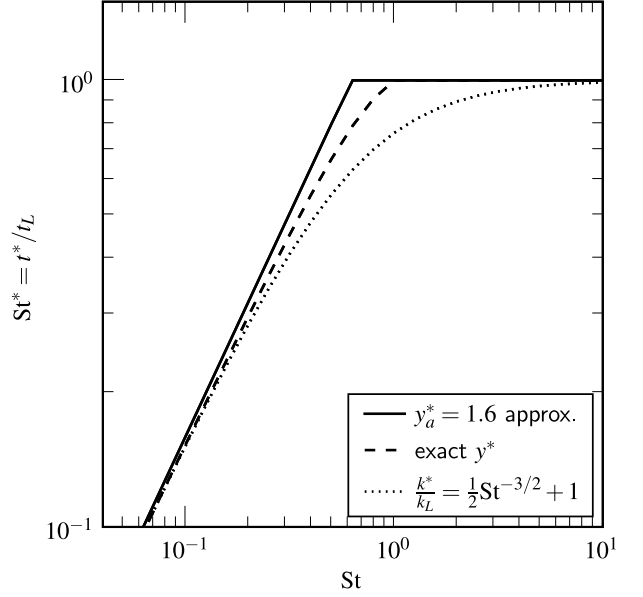


Fig. 2. Three different assumptions for t^* (or the related k^*) are shown here.

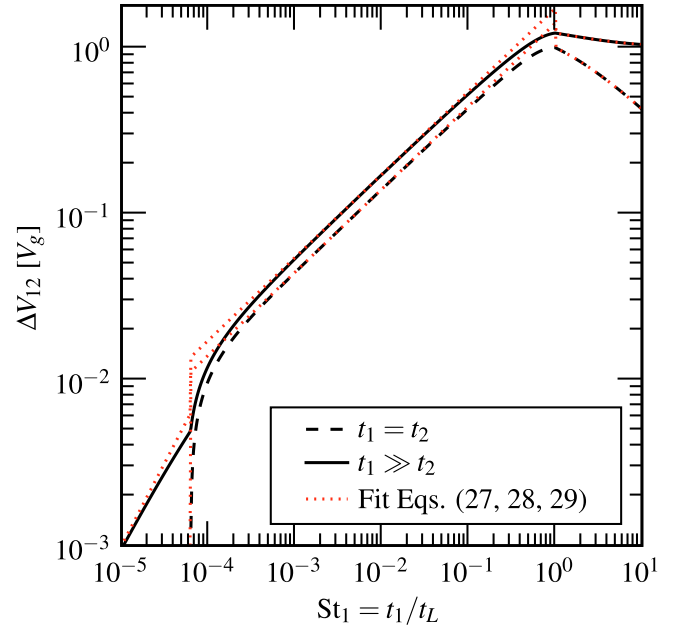


Fig. 3. Exact solution to Eq. (16) for ΔV_{12} in the case of identical particles (dashed line) and $t_1 \gg t_2$ (solid line) for a Reynolds number of 10^8 . The dotted curves are approximations to Eq. (16) given by Eqs. (27)–(29).

Cuzzi & Weidenschilling 2006). Then

$$\begin{aligned} \frac{V_o}{V_g} &= \frac{St}{St+1} \frac{\beta V_K}{\alpha^{1/2} c_g} = \frac{St}{St+1} \frac{\beta a \Omega}{\alpha^{1/2} H_g \Omega} \\ &= \frac{St}{St+1} \frac{\beta}{\alpha^{1/2} \beta^{1/2}} = \frac{St}{St+1} \left(\frac{\beta}{\alpha} \right)^{1/2}, \end{aligned} \quad (23)$$

and Eq. (22) becomes,

$$F(y^*) = \frac{St}{1+St} \left(\frac{\beta/\alpha}{1+St} - 1 \right). \quad (24)$$

Normally $\beta \sim 2 \times 10^{-3}$ is assumed (Nakagawa et al. 1986; Cuzzi et al. 1993), but its real value, and that of α , are not well known.

Equation (24) shows that for a given value of St , $F(y^*)$ increases with increasing β/α . Consequently, $y^* = t^*/t_s$ is also higher (see Fig. 1). The boundary between the class I and II eddies therefore shifts to higher values of t^* , that is, there are less class I eddies for high β/α and the $St^* = 1$ upper limit (when $t^* = t_L$) is reached at lower Stokes numbers. Inserting the definition of $F(y^*)$ (LHS of Eq. (22)) into Eq. (24) with $y^* = t_L/t_s = St^{-1}$ and solving for St , we find that the Stokes number at which $St^* = 1$ occurs at

$$St_{St^*=1} = \left(1 + \sqrt{\frac{3\beta}{2\alpha}}\right)^{-1/2}. \quad (25)$$

For example, for $\beta/\alpha = 1$, St^* reaches its upper limit at $St \approx 0.67$.

In the small particle regime ($St \ll 1$), however, the exact value of β/α is unimportant since $F(y^*)$ is always close to zero, and the y_a^* approximation is justified. It is only for $\beta/\alpha \gtrsim St^{-1}$ that the RHS of Eq. (24) starts to become significant and $y^* > y_a^*$. This is the weakly-turbulent or non-turbulent regime where class II eddies dominate even for small particles. In practise, however, it means that eddy crossing effects are important only if turbulence is very weak and we will not treat them further in this paper.

3.4. Limiting solutions

As intuition-building examples we obtain simple, closed-form expressions for ΔV_{12}^2 in various limiting regimes from the t -space solutions; similar results are easily obtained from the k -space solutions (Sect. 3.1). Without loss of generality we take particle 1 to have the largest stopping time, i.e., $t_1 \geq t_2$ and $t_{12}^* = t_1^*$. Moreover, we assume that $t_\eta \ll t_L$; i.e., that $Re^{1/2} \gg 1$ and there is an extended inertial range of eddies. Recall again that $St_{12}^* = Re^{-1/2}$ for $t_1 < t_\eta/y_a^*$, and that St_{12}^* will not exceed 1.

3.4.1. Tightly coupled particles, $t_1, t_2 < t_\eta$

In this limit all eddies are of class I and $\Delta V_{12}^2 \rightarrow \Delta V_1^2$. For each particle, the second term on the RHS of Eq. (17) is negligible; thus

$$\Delta V_{12}^2 = V_g^2 \frac{St_1 - St_2}{St_1 + St_2} \left(\frac{St_1^2}{St_1 + Re^{-1/2}} - \frac{St_2^2}{St_2 + Re^{-1/2}} \right). \quad (26)$$

In the very small particle regime ($t_1 \ll t_\eta$), $St_i \ll t_\eta/t_L = Re^{-1/2}$ and

$$\Delta V_{12}^2 = V_g^2 \frac{t_L}{t_\eta} (St_1 - St_2)^2. \quad (27)$$

Since $V_g^2 = \frac{3}{2} V_\eta^2 Re^{1/2} = \frac{3}{2} V_\eta^2 t_L/t_\eta$, this expression transforms directly to $\Delta V_{12} = \sqrt{3/2}(t_1 - t_2)V_\eta/t_\eta$, in good agreement with the heuristic, although physically motivated, expression $\Delta V_{12} = V_\eta(t_1 - t_2)/t_\eta$ of Weidenschilling (1984).

3.4.2. Intermediate regime, $t_\eta \leq t_1 \leq t_L$

If t_1 (the stopping time of the larger particle) approaches the Kolmogorov scale, two changes occur. First, the $St_1^2/(St_{12}^* + St_1)$ term in Eq. (17) now becomes linear with St_1 , since St_{12}^* grows proportional to St_1 (the second term is still negligible throughout most of this regime). Relative velocities therefore increase as the square-root of stopping time. Second, class II eddies also contribute to ΔV_{12}^2 (Eq. (18)). This contribution scales also with St_1 ,

but is significantly larger and does not disappear when $t_1 = t_2$. From a physical point of view, class II eddies act as small, random kicks to the particle trajectory, while two particles captured by a class I eddy are subject to the same, systematic, change in motion. Class II eddies are therefore much more effective in generating velocity differences for similar-sized particles.

In the ‘‘fully intermediate regime’’, i.e., $t_\eta \ll t_1 \ll t_L$, we can also ignore the $Re^{-1/2}$ terms in Eq. (18). In addition, the $t^*/t_s = y_a^*$ approximation holds. Upon writing $St_2 = \epsilon St_1$, Eqs. (17), (18) become linear with St_1 and we can write ΔV_{12}^2 as (see Appendix B)

$$\Delta V_{12}^2 = V_g^2 \left[2y_a - (1 + \epsilon) + \frac{2}{1 + \epsilon} \left(\frac{1}{1 + y_a} + \frac{\epsilon^3}{y_a + \epsilon} \right) \right] St_1, \quad (28)$$

where $\epsilon \leq 1$ is the ratio between the stopping times and $y_a = 1.6$. For $t_1 \gg t_2$ we then find that $\Delta V_{12}^2 \approx 3.0V_g^2 St_1$, while for equal particles the numerical factor goes down to 2.0. Written in terms of stopping times the relative velocities become, $\Delta V_{12} = [1.7 \div 2.1]V_L \sqrt{t_1/t_L}$. This also compares well with Weidenschilling (1984) fits for this regime (who gives pre-factors of 2.1 and 3.0, respectively). Note, however, that our full expressions for ΔV_{12} (Eqs. (16)–(18)) also capture the behavior near the t_η and t_L ‘‘turning points’’ (see Fig. 3).

3.4.3. Heavy particles, $t_1 > t_L$

If $t_1 > t_L$, $St_{12}^* = 1$ and there is no contribution from class I eddies (Eq. (17)). Also, we can neglect the $Re^{-1/2}$ terms in Eq. (18) and the relative velocity simply becomes

$$\Delta V_{12}^2 = \Delta V_{II}^2 = V_g^2 \left(\frac{1}{1 + St_1} + \frac{1}{1 + St_2} \right). \quad (29)$$

This result can, of course, directly be obtained from the V_{pi} terms (Eq. (12)) since the cross-term vanishes in this regime. For small St_2 relative velocities are still $\sim V_g$; however, if both Stokes numbers are large, the relative velocity decreases roughly with the square root of the smallest particle stopping time. Note that the linear fit of Weidenschilling (1984) in this regime (his Eq. (15)) is inappropriate (see, however, Völk et al. 1980, Weidenschilling 1988, Weidenschilling & Cuzzi 1993, Cuzzi et al. 1993, in which a square-root fall off is advocated). Since an explicit, closed-form solution to the Völk et al. (1980) and MMV expressions for ΔV_{12} has not previously been available, many dust coagulation models (e.g., Suttner & Yorke 2001; Dullemond & Dominik 2005; Ormel et al. 2007) have relied on the Weidenschilling (1984) fits to calculate relative velocities. Turbulent motions and relative velocities for particles in the $t_s > t_L$ regime have therefore been underestimated in these calculations. However, concerning these works, we also think no major conclusions have been affected, since the error is introduced only for large dust particles, that is, if the system is already well evolved.

3.5. Contour plots

Following Völk et al. (1980) and MMV we also present our results as contour plots. Figure 4A shows, for comparison, the results of MMV, obtained by numerical evaluation of the integrals involved without an inner turbulent scale ($Re \rightarrow \infty$). The next three panels of Fig. 4 show the result using our closed-form expressions derived from Eq. (16). In panel B, the y_a^* approximation has been used and, like Fig. 2 of MMV (panel A), the inner scale of the turbulence is extended to infinity so that

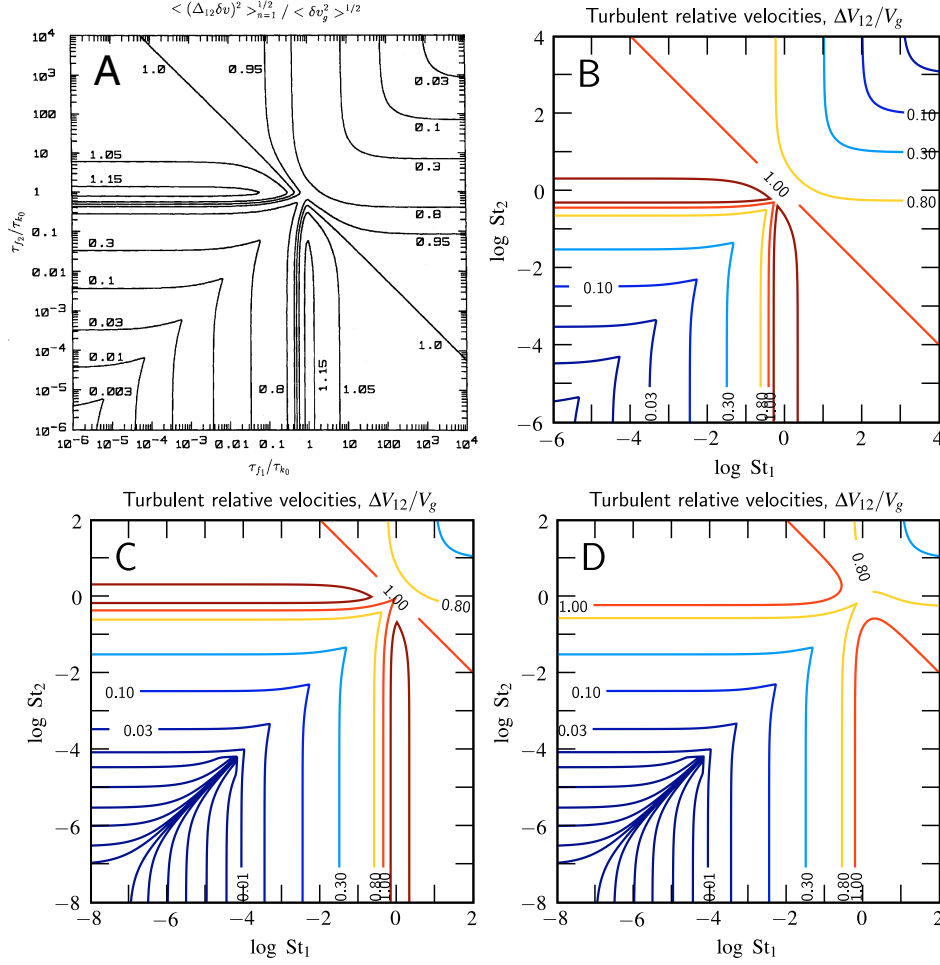


Fig. 4. Contour plots of particle-particle, turbulence induced, relative velocities ΔV_{12} normalized to V_g . **A)** Numerical results of Markiewicz et al. (1991), without inner scale ($Re \rightarrow \infty$). **B)** Analogous result from our closed-form expressions with the fixed $y_a^* \approx y_a^* = 1.6$ approximation (Sect. 3.2.1). **C)** Like B, but with an exact solution for y_a^* and with $Re = 10^8$. **D)** Using the CH03 formula for k^* , $k^*/k_L = 0.5St^* + 1$, and also with $Re = 10^8$. Contours are drawn twice per logarithmic decade (at $\Delta V_{12}/V_g = 3 \times 10^i$ and at 10^i) with an additional contour at 0.8 and 1.15.

Eqs. (28), (29) apply. Somewhat systematically higher values for ΔV_{12} when compared to MMV can be explained by the CH03 approximation for V_p (see Eq. (6)) but these discrepancies are less than $\sim 10\%$. In panels C and D we show the contour plots corresponding to the other formulations for k^* (see Fig. 2), i.e., the exact solution for y_a^* (panel C) and the CH03 empirical approximation (panel D). The differences between these three methods for determining k^* differ around the $St = 1$ point (see Fig. 2) and are reflected in the contour plots. For $St \approx 1$, panel C compares best to the numerical result of MMV, but no significant errors are made when using the y_a^* approximation or the CH03 formula for k^* .

In panels C and D of Fig. 4, a Reynolds number of $Re = 10^8$ has been adopted. For $St < 10^{-4}$, therefore, velocities are greatly suppressed since only class I eddies remain to generate relative velocities and relative velocities disappear completely for equal friction times. Also, the contours are much closer spaced since in this limit the velocity ΔV_{12} is proportional to St (see Eq. (26)).

4. Conclusions

We have extended and, essentially, completed the work of Cuzzi & Hogan (2003), who derived explicit, closed-form expressions for particle velocities in turbulence based on the physics originally developed by Völk et al. (1980) and

Markiewicz et al. (1991). Within the framework of this physics, the only approximations used here are in Eq. (6) for the particle velocities (where a posteriori comparisons with exact numerical solutions indicate the approximation is well justified) and in Eqs. (20) et seq where the systematic velocity V_0 is neglected to simplify calculating the boundary between eddy classes (generalizing this step should be straightforward, however). The full analytic expression for ΔV_{12} is given by Eq. (16) (or by the sum of Eqs. (17), (18)), but more simple, explicit expressions apply in restricted regimes (provided $Re^{1/2} \gg 1$):

- Equation (27), in the very small particle limit ($t_1 \ll t_\eta$);
- Equation (28), in the “fully intermediate” regime, i.e., for $t_\eta \ll t_1 \ll t_L$;
- Equation (29), for $t_1 \geq t_L$.

Near the $t_1 = t_\eta$ and $t_1 = t_L$ turning points the behavior is more complex (see Fig. 3) and for accurate analytical approximations one has to revert to the full expressions for ΔV given by Eqs. (16)–(18).

Acknowledgements. The authors thank Robert Hogan for computational assistance in creating Fig. A.1 and the referee, H. Völk, for positive feedback. C.W.O. acknowledges support from the Netherlands Organisation for Scientific Research (NWO) that made this work possible. J.N.C.’s contributions were supported by a grant from NASA’s Planetary Geology and Geophysics Program.

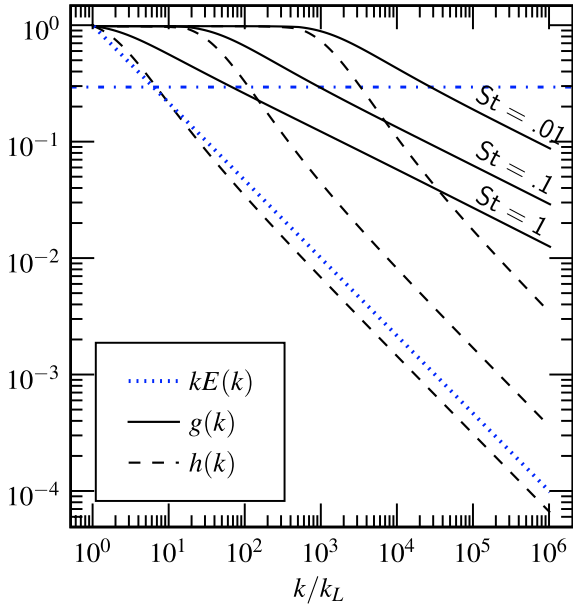


Fig. A.1. The functions g (solid lines) and h (dashed lines) plotted for three different Stokes numbers at a Reynolds number of 10^8 . After $k > k^*$ the functions show power-law behavior. The power spectrum (weighted by k) is plotted by the dotted line.

Appendix A: A more accurate closed-form solution for V_p and all related velocities, using power-law approximations to the functions g and h

In Sect. 2 the very simple approximation $g(\chi) = h(\chi) = 1$ was introduced for all Stokes numbers St and eddy scales k . It proves to be quite adequate for most purposes; however, as noted in Sect. 3.5, small inaccuracies remain at the 10% level because the approximation overestimates the contributions of fast eddies to V_p^2 and other velocity components. Figure A.1 shows the detailed behavior of the functions g and h for $Re = 10^8$ for Stokes numbers of $St = 0.01, 0.1$, and 1.0 . The inflection point for all three values of St is at $k = k^*$ (recall that $k^*/k_L \approx 1 + \frac{1}{2}St^{-3/2}$). For $k > k^*$, the functions are well approximated by power-laws of $-1/3$ and $-3/4$, respectively, i.e., $g(k) = (k/k^*)^{-1/3}$ and $h(k) = (k/k^*)^{-3/4}$. The success of the approximation of Sect. 2 is due to the fact that the power in the weighting function $kE(k)$ (dotted line; we multiply with k since we compare logarithmically) decreases rapidly with increasing k ; thus by the time the assumption $g(k) = h(k) = 1$ becomes really bad, the relative contribution of successive terms has become small. For small St , the weighted contribution of eddy power has already become very small even before $k \sim k^*$ (the logic of CH03). For $St = 1$ or larger, the weighting function has dropped by nearly an order of magnitude by the time $h(k)$ (the faster-decreasing function) has dropped to 0.3 (dashed-dotted line), and this seems to account for the success of our simple assumption.

This behavior can be understood from the definition of $\chi = Kt_k k V_{rel}$. For $k \gg k^*$, $K \approx 1$ and $V_{rel} \lesssim V_g$ are both constant. Then, because $t_k \propto k^{-2/3}$, χ scales as $\chi \propto k^{1/3}$ and becomes large at large k . Since $g(\chi) = \arctan(\chi)/\chi \propto \chi^{-1}$ for large χ , we get that $g(k) \propto k^{-1/3}$. Similarly, $h(\chi) \propto k^{-2/3}$, which is a bit shallower than the $-3/4$ exponent observed over most regions of interest (Fig. A.1). While the $-2/3$ exponent is reached at large k , the

$-3/4$ exponent seems more appropriate at intermediate k . Yet, in our subsequent analysis, we will use the large- k limit for this exponent ($-2/3$) because it simplifies the math. Thus, we approximate the g and h behavior as follows: unity for $k < k^*$, and power laws in k/k^* with exponents of $-1/3$ and $-2/3$ for $k > k^*$. Then Eq. (4) becomes

$$V_p^2 = \int_{k_L}^{k^*} dk 2E(k) (1 - K^2) + \int_{k^*}^{k_\eta} dk 2E(k) (1 - K) \left[\left(\frac{k}{k^*} \right)^{-1/3} + K \left(\frac{k}{k^*} \right)^{-2/3} \right]. \quad (\text{A.1})$$

Where we have that $k_L \leq k^* \leq k_\eta$, such that in the case of very small or very large particles one of the integrals vanishes (Sect. 3.2.1). Since the approximation $g = h = 1$ still holds for $k < k^*$ (or for $t > t^*$) the velocities resulting due to class 1 eddies (Eq. (17)) are not affected; the new approximation only affects Eq. (18). By writing $K = St/(St + x^{-2/3})$, $E(k) = E_L(k/k_L)^{-5/3} \propto x^{-5/3}$ with $x = k/k_L$ the solution to Eq. (A.1) involves integrals of the form

$$\int dx x^{-5/3+p} \left(\frac{St}{St + x^{-2/3}} \right)^{n=[1, 2]} \quad (\text{A.2})$$

with $n = 2$ for the K^2 term and $p = -1/3$ or $-2/3$. These integrals can be solved analytically. Going to “ t -space”, however, gives somewhat cleaner solutions and we will from here on follow that approach and show how it affects relative velocities, i.e., ΔV_{II} . After the change of variables ($t_k/t^* = (k/k^*)^{-2/3}$) the second term of Eq. (A.1) becomes

$$\frac{V_g^2}{t_L} \int_{t_\eta}^{t^*} dt_k (1 - K) \left(\frac{t_k}{t^*} \right)^{1/2} + (1 - K) K \left(\frac{t_k}{t^*} \right). \quad (\text{A.3})$$

We now introduce the dimensionless variable $y = t_k/t_s$ (cf. Eq. (20)). Then $t_k/t^* = y/y^*$ with $y^* = t^*/t_s$. Also $K = 1/(1 + y)$ and $1 - K = y/(1 + y)$ and Eq. (A.3) becomes

$$\frac{V_g^2 t_s}{t_L} \int_{t_\eta/t_s}^{t^*/t_s} dy (y^*)^{-1/2} \frac{y^{3/2}}{1 + y} + (y^*)^{-1} \frac{y^2}{(1 + y)^2} = \quad (\text{A.4})$$

$$\frac{V_g^2 t_s}{t_L} \left\{ (y^*)^{-1/2} \left[I_h(y) \right]_{t_\eta/t_s}^{t^*/t_s} + (y^*)^{-1} \left[I_g(y) \right]_{t_\eta/t_s}^{t^*/t_s} \right\} \quad (\text{A.5})$$

in which the functions $I_h(y)$ and $I_g(y)$ are defined as

$$I_h(y) \equiv \int_0^y dz \frac{z^{3/2}}{1 + z} = \left(\frac{2}{3}y - 2 \right) \sqrt{y} + 2 \arctan(\sqrt{y}) \quad (\text{A.6})$$

$$I_g(y) \equiv \int_0^y dz \frac{z^2}{(1 + z)^2} = \frac{(2 + y)y}{1 + y} - 2 \log(1 + y). \quad (\text{A.7})$$

The expressions for ΔV_{II} now consist of several contributions. First, $I_h(y)$ and $I_g(y)$ are evaluated at both the upper (y^*) and lower (y_η) limits. This must be done for both particles 1 and 2, because the ΔV_{II} term (Eq. (18)) has separate contributions from each particle. For the particle of highest friction time (say this is t_1) the power-law approximation for g and h holds over the range ΔV_{II} is calculated, i.e., $t_s \leq t_{1k} \leq t_{12}^* = t_1^*$. However, for the second particle the power-law approximation only holds for $t_{2k} \leq t_2^*$, while for the remaining range over which the integral in ΔV_{II} is evaluated, i.e., $t_2^* \leq t_{2k} \leq t_1^*$, the $g = h = 1$ approximation applies.

This gives us several terms that contribute to ΔV_{II} . Collecting these terms, the new expression for ΔV_{II} becomes

$$\begin{aligned} \Delta V_{II} = & \frac{V_g^2}{t_L} \left\{ t_1 \left(\frac{t_1^*}{t_1} \right)^{-1/2} \left[I_h(y) \right]_{t_\eta/t_1}^{t_1^*/t_1} + (1 \leftrightarrow 2) \right. \\ & + t_1 \left(\frac{t_1^*}{t_1} \right)^{-1} \left[I_g(y) \right]_{t_\eta/t_1}^{t_1^*/t_1} + (1 \leftrightarrow 2) \\ & \left. + \left[t_k + \frac{t_2^2}{t_2 + t_k} \right]_{t_2^*}^{t_1^*} \right\}, \quad (t_1 \geq t_2). \end{aligned} \quad (\text{A.8})$$

Although still fully analytical, this more accurate expression for ΔV_{II} is also more complicated and we did not present it in the main body of the paper. Equation (A.8) is useful, however, for readers whose applications demand this higher level of accuracy.

Appendix B: Derivation of Eq. (28)

We consider the limiting case of $t_\eta \ll t_1 \ll t_L$. The y_a^* approximation for St_{12}^* then holds, i.e., $St_{21}^* \approx y_a^* St_1$ with $y_a = 1.6$. We will now argue that we can neglect the $Re^{-1/2}$ terms in Eq. (18). For particle 1 this is obvious since $St_1 \gg Re^{-1/2}$. The last term (where $Re^{-1/2}$ is in the denominator) then becomes simply $-St_1$. However, for the interchange term a similar approximation

$$\frac{St_2^2}{St_2 + Re^{-1/2}} \approx St_2, \quad (\text{B.1})$$

is not that obvious since we have not put a constraint on St_2 . For example, if $St_2 \ll Re^{-1/2}$ the $Re^{-1/2}$ term dominates the denominator. However, in that case this term *and* its approximation are small anyway compared to $-St_1$, such that by making the approximation in Eq. (B.1) our final result is not

affected. Similarly, if $St_2 \sim Re^{-1/2}$, Eq. (B.1) (which goes to $\sim \frac{1}{2} Re^{-1/2}$) or its approximation ($\sim Re^{-1/2}$) are insignificant since $St_1 \gg Re^{-1/2}$. Only if $\epsilon \sim 1$, i.e., $St_2 \gg Re^{-1/2}$, does the St_2 term matter, but then the approximation in Eq. (B.1) is well justified. All terms in Eq. (18) are then linear in Stokes and we can reduce it to

$$\frac{\Delta V_{II}^2}{V_g^2} = \left(2y_a^* - (1 - \epsilon) + \frac{1}{1 + y_a^*} + \frac{\epsilon^2}{\epsilon + y_a^*} \right) St_1, \quad (\text{B.2})$$

with $\epsilon = St_2/St_1 \leq 1$. Similarly, Eq. (17) becomes

$$\frac{\Delta V_I^2}{V_g^2} = \frac{1 - \epsilon}{1 + \epsilon} \left(\frac{1}{y_a^* + 1} - \frac{\epsilon^2}{y_a^* + \epsilon} \right) St_1. \quad (\text{B.3})$$

Combining these expressions and collecting the $1/(1 + y_a^*)$ and $\epsilon^2/(y_a^* + \epsilon)$ terms then gives Eq. (28).

References

- Cuzzi, J. N., & Hogan, R. C. 2003, *Icarus*, 164, 127
 Cuzzi, J. N., Dobrovolskis, A. R., & Champney, J. M. 1993, *Icarus*, 106, 102
 Cuzzi, J. N., & Weidenschilling, S. J. 2006, *Particle-Gas Dynamics and Primary Accretion, Meteorites and the Early Solar System II*, 353
 Dullemond, C. P., & Dominik, C. 2005, *A&A*, 434, 971
 Markiewicz, W. J., Mizuno, H., & Völk, H. J. 1991, *A&A*, 242, 286
 Nakagawa, Y., Sekiya, M., & Hayashi, C. 1986, *Icarus*, 67, 375
 Nomura, H., & Nakagawa, Y. 2006, *ApJ*, 640, 1099
 Ormel, C. W., Spaans, M., & Tielens, A. G. G. M. 2007, *A&A*, 461, 215
 Schräpler, R., & Henning, T. 2004, *ApJ*, 614, 960
 Suttner, G., & Yorke, H. W. 2001, *ApJ*, 551, 461
 Völk, H. J., Morfill, G. E., Roeser, S., & Jones, F. C. 1980, *A&A*, 85, 316
 Weidenschilling, S. J. 1984, *Icarus*, 60, 553
 Weidenschilling, S. J. 1988, *Formation processes and time scales for meteorite parent bodies, Meteorites and the Early Solar System*, 348
 Weidenschilling, S. J., & Cuzzi, J. N. 1993, in *Protostars and Planets III*, ed. E. H. Levy, & J. I. Lunine, 1031